

# Scan Angle Extension by Array with Pattern Reconfigurable Elements

S. Xiao, Y.-Y. Bai, B.-Z. Wang, and S. Gao

Institute of Applied Physics, University of Electronic Science and Technology of China,  
Chengdu, 610054, P. R. China  
xiaoshaoqiu@uestc.edu.cn

**Abstract** – In this paper, a linear phased array with pattern reconfigurable elements is studied to perform a scan angle extension of the array. The developed array can scan its main beam from  $-70^\circ$  to  $70^\circ$  in its scanning plane. Compared with the traditional microstrip phased array, the scanning angle is extended remarkably.

**Keywords:** Microstrip phased array, scan angle extension, and pattern reconfigurable antenna.

## I. INTRODUCTION

Phased array can scan its beam and provide a high gain, which results in its extensive applications. Microstrip antenna is utilized frequently in array because they have a compact and stable structure as well as the merit of easy installation [1-3]. There are two main factors to influence the pattern scan of the microstrip array. One is the mutual coupling between elements. Many researchers have studied on this topic and some valuable techniques have been developed to effectively suppress the element mutual coupling, such as using photonic bandgap (PBG) structure and Defected Ground Structure (DGS) [4-7]. The other is the directivity of the element pattern. Generally, the main beam of the microstrip antenna directs to the normal of the element aperture and faint energy is radiated into the space close to the tangent of the ground plane. Thus, when such elements are used to construct a planar phased array, the array cannot also radiate the energy to a large angle away from the normal of the array aperture. However, in some applications, for example, military radar for target scout, it is desired to scan the beam of the phased array in full space. Currently, how to extend the scan angle of the array is becoming a challenge topic in the planar microstrip phased array study.

Reconfigurable antenna has been presented and its operation characteristics, such as patterns and frequencies, are switchable by using PIN diodes or

MEMS switches [8-11]. Due to the ability of reconfiguring pattern, the reconfigurable antenna can improve the beam coverage range of the element pattern. Then the phased array constructed by the pattern reconfigurable antenna has a tremendous potential to extend the scan angle. The array with pattern reconfigurable elements has been studied by J. T. Bernhard et al firstly [12]. In [12], the characteristic of the pattern scan is compared between the proposed array and the traditional microstrip array. However, the reported array has a smaller scan range because of the incompact element configuration and the larger element spacing.

In this paper, an improved reconfigurable antenna element is applied into a linear phased array to extend the scan angle. Compared with the traditional microstrip array, the scanning angle of the developed array is extended remarkably.

## II. ANTENNA ELEMENT DESIGN

The element is a pattern reconfigurable microstrip dipole Yagi antenna and its geometry is shown in Fig. 1. The antenna consists of three parallel microstrip dipoles. The width of the microstrip dipole is  $W=2\text{mm}$ . The center strip length is  $L_m=20.6\text{mm}$ , and fed by a SMA connector. The feed position is moved  $g=8.5\text{mm}$  away from the end of the strip. The two parasitic microstrip dipoles have a same length of  $L_r=22.7\text{mm}$ . The space between the adjacent dipoles is  $S=9.8\text{mm}$ . A gaps with a width of  $d_m=1.2\text{mm}$  is located close to each end of the parasitic dipole and  $2.0\text{mm}$  ( $d_1$ ) away from the strip end. Four switches, i.e.,  $k_1$ ,  $k_2$ ,  $k_3$ , and  $k_4$ , are installed in four gaps, respectively. The ground plate has an area of  $100\times 140\text{mm}^2$ . The microstrip substrate have a relative permittivity of  $\epsilon_r=4.4$  and a thickness of  $H=6.35\text{mm}$ .

The antenna can reconfigure its pattern with three states. In *State 1*,  $k_1$  and  $k_2$  are open,  $k_3$  and  $k_4$  are closed. In this case, the right parasitic microstrip dipole is

shorten by opening k1 and k2 and the left one is elongated by closing k3 and k4. On the contrary, when k1 and k2 are closed, k3 and k4 are open, the configuration of *State 2* is realized.

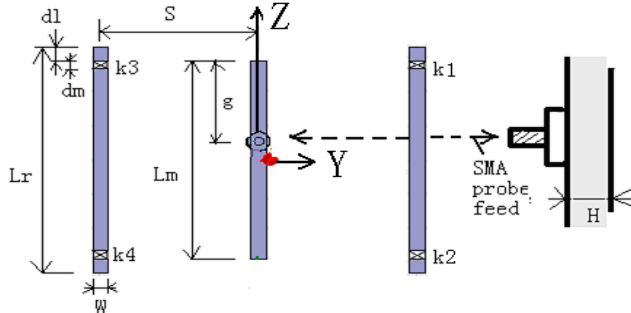


Fig. 1. Geometry of the pattern reconfigurable antenna element.

In this study, an ideal switch models are used to imitate PIN diode or MEMS switches for proof of concept, i.e., the open or closed states of the switches are imitated with the absence or presence of a metal pad with an area of  $W \times d_m$ . This simplification is acceptable because simulation and measurement show that the mutual coupling between antenna and radiation behavior change little after adding the switches and bias network [13-14]. The electromagnetic simulation software Ansoft HFSS 9.0 is used to study the antenna performances. The antenna that operates in *State 1* is analyzed firstly. The simulated and measured return losses are shown in Fig. 2. A good matching performance is achieved at the frequency of 3.67GHz.

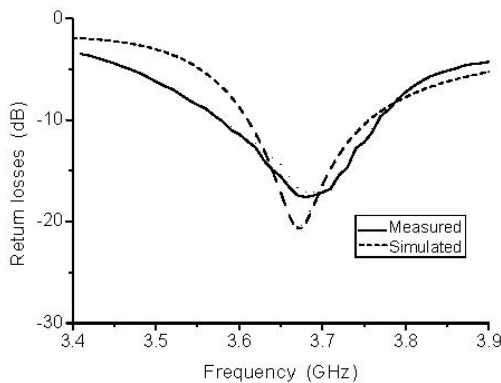


Fig. 2. Simulated and measured return losses for *State 1*.

Because the antenna is fed asymmetrically, the peak direction of radiation pattern is not in  $xy$ -plane when the antenna operates at 3.67GHz. A peak gain of 4.1dBi is obtained at the direction of  $(\theta=98^\circ, \varphi=2^\circ)$ , which is less

than the reported one in [15] because of a compacter antenna structure. The maximum radiation angle in  $\theta=90^\circ$  ( $xy$ -plane) is  $\varphi=44^\circ$ . The simulated and measured co-polarization patterns in  $\theta=90^\circ$  plane and  $\varphi=44^\circ$  plane are shown in Fig. 3. Here, the weak  $x$ -polarization components are omitted. The corresponding peak gain in Fig. 3 is 2.1dBi. Because the structure of *State 2* is symmetrical with that of *State 1*, the results for *State 2* are not shown by figures. The corresponding data of two states are listed in Table 1. Form Table 1, it can be shown that the antenna can reconfigure its pattern in  $xy$ -plane with an acceptable antenna gain by shifting antenna states between *State 1* and *State 2*.

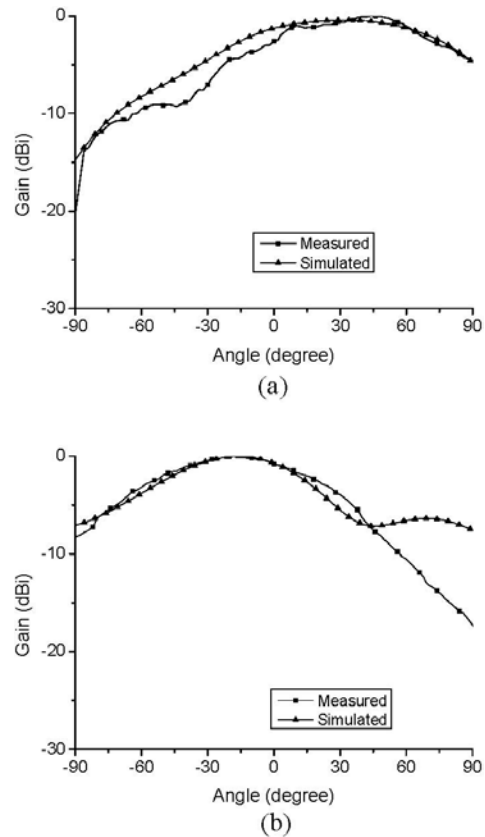


Fig. 3. Simulated and measured radiation patterns at 3.67 GHz in (a)  $\theta=90^\circ$  plane ( $xy$ -plane) and (b)  $\varphi=-44^\circ$  plane for *State 1*.

Table 1. Relative data for pattern reconfigurable antennas.

State	Maximum radiation direction		Beam coverage in $xy$ -plane		Gain	
	full space	$xy$ -plane	3dB	6dB	Full space	$xy$ -plane
1	(52°, 25°)	(90°, 40°)	27° ~ 53°	-50° ~ 79°	4.6	2.2
2	(52°, -25°)	(90°, -40°)	-53° ~ -27°	-79° ~ -50°	4.6	2.2

### III. LINEAR PHASED ARRAY FOR SCAN ANGLE EXTENSION

The geometry of the proposed linear phased array is shown in Fig. 4. Eight elements, named *no.1-no. 8*, are arranged along *y*-axis with element space of  $d=\lambda/2$ , where  $\lambda$  is the wavelength in free space at the operation frequency. The array has a ground plane with an area of  $100\text{mm}\times 420\text{mm}$ . All of the elements in the phased array operate with the same state and are fed with the same signal amplitude. When the elements in array operate with *State 1*, the simulated return loss at each port and the simulated mutual couplings between two adjacent elements ( $S_{mn}$  with  $|m-n|=1$ ) are shown in Fig. 5. In this figure, it can be observed that a return loss of  $-30\text{dB}$  is achieved for each port and a mutual coupling of less than  $-20\text{dB}$  is obtained between the adjacent elements at the operation frequency of  $3.67\text{GHz}$ . Based on the simulation, the mutual coupling between other elements is decreased further due to larger element spacing. When the elements in array operate in *State 2*, the array performances can be deduced according to the symmetry of the geometry between *State 1* and *State 2*.

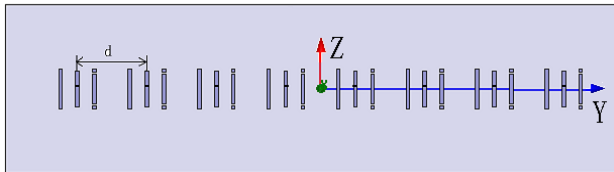


Fig. 4. Geometry of the linear phased array constructed by pattern reconfigurable antenna elements.

The mutual coupling between elements in array can influence severely the array performances. Generally speaking, it can lead to two problems. One is that the active reflection coefficient at each port is increased remarkably when the scan angle away from the array normal is large; and the other is to create the scan blindness in some special angles. Based on the scattering parameter matrix of the array, the active reflection coefficient at each port can be calculated by the following formula,

$$T_m(\theta) = \frac{V_m^{out}}{V_m^{in}} = e^{jkmd \sin \theta} \sum_{n=1}^N S_{mn} e^{-jknd \sin \theta} \quad (1)$$

where  $m$  is the element number,  $\theta$  is the array scan angle and  $N$  is the total of the element. The calculated active

reflection coefficients at *Port 1, Port 2, Port 3* and *Port 4* are shown in Fig. 6. It can be observed that a weak active reflection is generated at ports even if the scan angle is large and no total reflection, i.e., no scan blindness, occurs within  $\varphi=0^\circ-90^\circ$ .

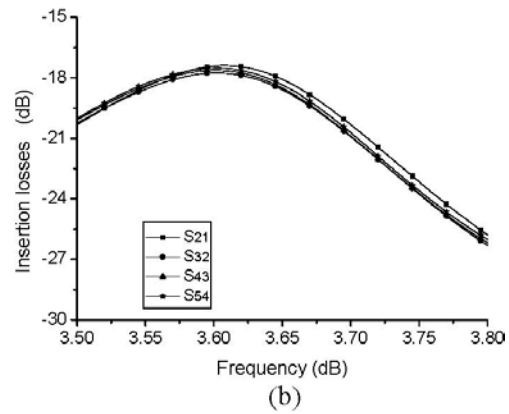
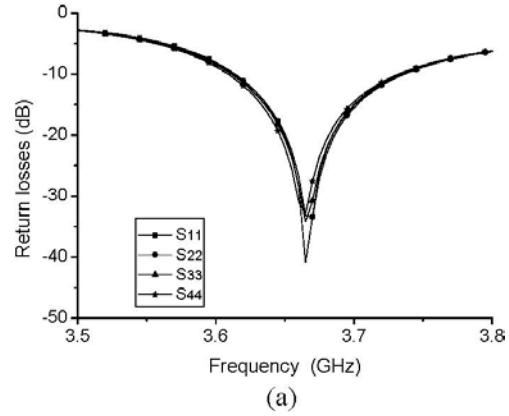


Fig. 5. Simulated (a) return losses at each port and (b) mutual coupling between adjacent elements.

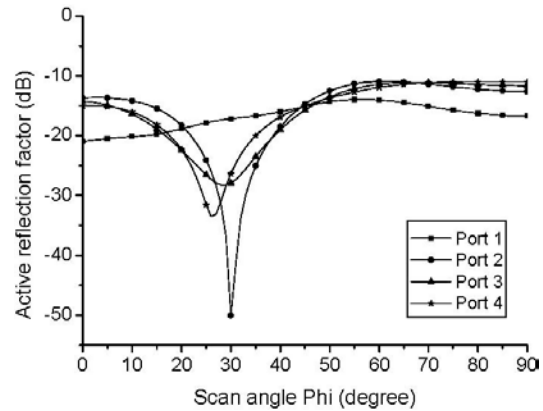


Fig. 6. Simulated active reflection coefficient at feed ports.

The radiation characteristics of the phased array are analyzed by Ansoft HFSS. The progressive phase between two adjacent elements is  $\Delta\psi$ . Figure 7(a) demonstrates the patterns of the array in  $xy$ -plane when the elements operate in *State 1* and with various progressive phases. The results indicate that, as increasing the progressive phase  $\Delta\psi$ , the scan angle can move from the array normal ( $x$ -axis) toward the large angle close to the ground ( $y$ -axis) with a good gain performance. The patterns in called plane which is orthogonal to  $xy$ -plane and passes through the maximum radiation angle in  $xy$ -plane, are plotted in Fig. 7(b).

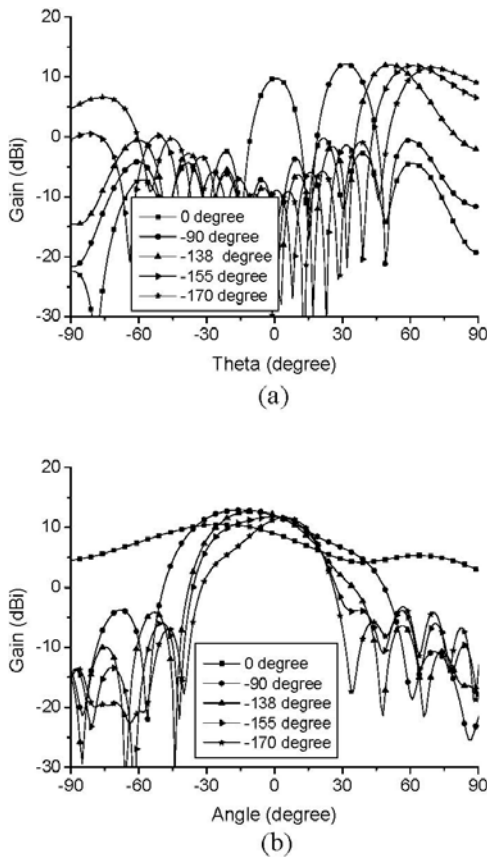


Fig. 7. Radiation pattern of the linear phased array when elements operate in *State 1* and with various progressive phases, (a)  $xy$ -plane and (b)  $E$ -plane.

The figure shows that the phased array can scan its patterns from  $\varphi = -70^\circ$  to  $70^\circ$  in  $xy$ -plane. Based on the symmetry, when the elements in the array operate in *State 2* the array performance can be deduced. All of the detailed data of the array scan performance are shown in Table 2. From Table 2, we can observe that the developed linear phased array can scan its patterns from  $\varphi = -70^\circ$  to

$70^\circ$  in  $xy$ -plane and provide a full angle coverage with 3-dB beam width and good gain performance. Like the single element, the maximum radiation direction of the array is not in  $xy$ -plane, however, an acceptable gain performance is achieved when the phased array performs its pattern scan in  $xy$ -plane.

Table 2. Pattern scan characteristic of the developed array with various progressive phases.

$\Delta\psi$	Direction( $\theta_0, \phi_0$ )		Beam coverage in $xy$ -plane		Gain (dBi)	
	Aim	Maximum	3dB	6dB	$xy$ -plane	Full space
<i>State 1</i>						
$0^\circ$	$(90^\circ, 0^\circ)$	$(46^\circ, 0^\circ)$		$-4^\circ \sim 5^\circ$	7.26	11.3
$-20^\circ$	$(90^\circ, 7^\circ)$	$(46^\circ, 10^\circ)$		$2^\circ \sim 12^\circ$	7.22	11.2
$-40^\circ$	$(90^\circ, 14^\circ)$	$(47^\circ, 19^\circ)$		$9^\circ \sim 19^\circ$	7.4	11.2
$-60^\circ$	$(90^\circ, 21^\circ)$	$(55^\circ, 25^\circ)$	$19^\circ \sim 24^\circ$		8.52	11.1
$-70^\circ$	$(90^\circ, 25^\circ)$	$(54^\circ, 30^\circ)$	$22^\circ \sim 27^\circ$		8.92	11.52
$-90^\circ$	$(90^\circ, 32^\circ)$	$(59^\circ, 37^\circ)$	$28^\circ \sim 35^\circ$		9.58	11.70
$-110^\circ$	$(90^\circ, 39^\circ)$	$(73^\circ, 41^\circ)$	$34^\circ \sim 45^\circ$		9.9	11.93
$-138^\circ$	$(90^\circ, 51^\circ)$	$(76^\circ, 52^\circ)$	$46^\circ \sim 57^\circ$		9.74	11.82
$-155^\circ$	$(90^\circ, 61^\circ)$	$(85^\circ, 60^\circ)$	$51^\circ \sim 77^\circ$		9.97	11.04
$-170^\circ$	$(90^\circ, 70^\circ)$	$(92^\circ, 70^\circ)$	$57^\circ \sim 90^\circ$		10.27	10.57
<i>State 2</i>						
$0^\circ$	$(90^\circ, 0^\circ)$	$(46^\circ, 0^\circ)$		$-5^\circ \sim 4^\circ$	7.26	11.3
$20^\circ$	$(90^\circ, -10^\circ)$	$(46^\circ, -10^\circ)$		$-12^\circ \sim 2^\circ$	7.22	11.2
$35^\circ$	$(90^\circ, -17^\circ)$	$(47^\circ, -19^\circ)$		$-19^\circ \sim 9^\circ$	7.4	11.2
$60^\circ$	$(90^\circ, -21^\circ)$	$(55^\circ, -25^\circ)$	$-24^\circ \sim 19^\circ$		8.52	11.1
$70^\circ$	$(90^\circ, -25^\circ)$	$(54^\circ, -30^\circ)$	$-27^\circ \sim 22^\circ$		8.92	11.52
$90^\circ$	$(90^\circ, -32^\circ)$	$(59^\circ, -37^\circ)$	$-35^\circ \sim 28^\circ$		9.58	11.70
$110^\circ$	$(90^\circ, -39^\circ)$	$(73^\circ, -41^\circ)$	$-45^\circ \sim 34^\circ$		9.9	11.93
$138^\circ$	$(90^\circ, -51^\circ)$	$(76^\circ, -52^\circ)$	$-57^\circ \sim 46^\circ$		9.74	11.82
$155^\circ$	$(90^\circ, -61^\circ)$	$(85^\circ, -60^\circ)$	$-77^\circ \sim 51^\circ$		9.97	11.04
$170^\circ$	$(90^\circ, -70^\circ)$	$(92^\circ, -70^\circ)$	$-90^\circ \sim 57^\circ$		10.27	10.57

IV. CONCLUSION

A linear phased array with pattern reconfigurable elements is proposed in this paper. The pattern reconfigurable element operates in two switchable states with good performances. The developed linear phased array can perform its pattern scan from  $\varphi = -72^\circ$  to  $72^\circ$  in  $xy$ -plane and provide a full angle coverage with 3-dB beam width and acceptable gain performance. This study validates the validity of extending the scan angle of the phased array by using the pattern reconfigurable antenna element.

## ACKNOWLEDGEMENT

This work was in part supported by aviation Science foundation under grant 20070180003, in part by the new-century talent program of the education department of China under grant NCET070154, in part by national defense research funding under grant 08DZ0229 and in part by the national natural science foundation of China under grant No 60872034.

## REFERENCES

- [1] R. Staraj, E. Cambiaggio, and A. Papiernik, "Infinite phased arrays of microstrip antennas with parasitic elements: application to bandwidth enhancement," *IEEE Trans. on Antennas and Propagation*, vol. 42, no. 5, pp. 742-746, 1994.
- [2] A. K. Skrivervic and J. R. Mosig, "Finite phased array of microstrip patch antennas: the infinite array approach," *IEEE Trans. on Antennas and Propagation*, vol. 40, no. 5, pp. 579-582, 1992.
- [3] G. T. Javier, F. W. Parveen, T. C. Michael, and G. C. Christos, "FDTD analysis of finite-sized phased array microstrip antennas," *IEEE Trans. on Antennas and Propagation*, vol. 51, no. 8, pp. 2057-2062, 2003.
- [4] Z. Iluz, R. Shavit, and R. Bauer, "Microstrip antenna phased array with electromagnetic bandgap substrate," *IEEE Trans. on Antennas and Propagation*, vol. 52, no. 6, pp. 1446-1453, 2004.
- [5] Yunqi Fu and Naichang Yuan, "Elimination of scan blindness in phased array of microstrip patches using electromagnetic bandgap materials," *IEEE Antennas and Wireless Propagation Letters*, vol. 3, pp. 63-65, 2004.
- [6] F. Yang and Y. Rahmat-Samii, "Microstrip antennas integrated with electromagnetic band-gap (EBG) structures: a low mutual coupling design for array applications," *IEEE Trans. Antennas Propagat.*, vol. 51, no. 10, pp. 2936-2946, Oct. 2003.
- [7] D.-B. Hou, S. Q. Xiao, B.-Z. Wang, L. Jiang, J. Wang, and W. Hong, "Scan blindness elimination with compact DGSSs in microstrip phased array," Accepted by *IET Microwaves, Antennas & propagation*, 2008.
- [8] S. Q. Xiao, Z. H. Shao, M. Fujise, and B.-Z. Wang, "Pattern reconfigurable leaky-wave antenna design by FDTD method and Floquet's theorem," *IEEE Trans. Antennas Propagate.*, vol. 53, no. 5, pp. 1845-1848, May 2005.
- [9] Yang and Y. Rahmat-Samii, "Patch antennas with switchable slots (PASS) in wireless communications: Concepts, designs, and applications," *IEEE Antennas and Propagation Mag.*, vol. 47, no. 2, pp. 13-29, April 2005.
- [10] D. Peroulis, Kamal Sarabandi, and L. P. B. Katehi, "Design of Reconfigurable Slot Antennas," *IEEE Trans. Antennas Propagate.*, vol. 53, no. 2, pp. 645-654, Feb. 2005.
- [11] J. Zhang and A. Wang, "A survey on reconfigurable antennas," *Microwave and Millimeter Wave Technology International Conference, ICMMT 2008*, vol. 3, pp. 1156-1159, April 2008.
- [12] S. Zhang and J. T. Bernhard, "Performance study of a reconfigurable microstrip parasitic array (RMPA) phased array," *2006 IEEE Antennas and Propagation Society International Symposium*, pp. 2305-2308, 2006.
- [13] F. Yang and Y. Rahmat-Samii, "Patch antenna with switchable slot (PASS): dual frequency operation," *Microwave and Optical Technology Letters*, vol. 31, pp. 165-168, 2001.
- [14] J. Kiriazi and H. Ghali, "Reconfigurable dual-band dipole antenna on silicon using series MEMS switches," *IEEE Antennas and Propagation Society International Symposium 2003*, pp. 403-406, 2003.
- [15] S. Zhang, G. H. Huff, J. Feng, and J. T. Bernhard, "A pattern reconfigurable microstrip parasitic array," *IEEE Trans. on Antennas and Propagation*, vol. 52, no. 10, pp. 2773-2776, 2004.